Journal of Chromatography, 597 (1992) 167–172
Elsevier Science Publishers B.V., Amsterdam

CHROM. 23 867

Kinetic aspects of membrane-based immunoaffinity chromatography

Michele Nachman

Department of Protein Biochemistry, Roche Research Center, Hoffmann-La Roche Inc., Nutley, NJ 07110 (USA)

ABSTRACT

With a view towards the efficient large-scale purification of recombinant proteins, factors influencing antigen–antibody adsorption kinetics were studied in a model hollow-fiber membrane-based immunosorbent. Non-diffusion-controlled, homogeneous adsorption kinetics are approached in membranes. It is shown that adsorption kinetics, rather than mass transfer, first becomes limiting in membrane-based immunoaffinity chromatography (MIC). Antigen adsorption is not kinetically limited, even at low feed-stream antigen concentrations. Binding efficients approach theoretical values when antibody coupling densities are decreased sufficiently. Antigen breakthrough during adsorption occurs near the membrane's observed binding capacity. The results of these kinetic studies were essential in the development of highly efficient and productive MIC systems for the purification of three recombinantly produced biotherapeutics, interferon-α2a, interleukin-2 and interleukin-2 receptor.

INTRODUCTION

The two potential rate-limiting factors in affinity chromatography are mass transfer and adsorption kinetics. Both must be maximized for the system to be efficient. As immunoaffinity chromatography involves high affinity antigen–antibody (Ag–Ab) interactions, it is mass transfer which first becomes limiting in diffusion-controlled particle-based systems. Consequently, the fast Ag–Ab adsorption kinetics are often not maximally utilized. The diffusion time, t_D, must be much smaller than the residence time, t_R, of the antigen in the support matrix. As t_D is directly related to the diffusional distance, L,

$$t_D = L^2/D$$

the extremely short diffusional distance (< 1 μm) in membranes results in negligible diffusional limitations [1]. This enables one to study the kinetic limitations in membrane-based immunoaffinity chromatography (MIC). In fact, non-diffusion-controlled solution kinetics are approached in membrane-based systems, the difference being that the antibodies are on a membrane surface.

Assuming that membrane systems are analogous to free solution, antigen-antibody adsorption kinetics in MIC can be predicted by the rate expression

$$\frac{d\,[Ab \cdot Ag]}{dt} = k_1\,[Ab][Ag] - k_{-1}\,[Ab \cdot Ag] \quad (1)$$

As k_{-1} is very small compared with k_1, the primary factors that determine the extent of antigen capture in an immunosorbent are [Ab], [Ag] and k_1.

Antigen–antibody adsorption kinetics in an immobilized system can also be described in terms of the effective dissociation constant, K_{de}, which is defined as [2]

$$K_{de} = \frac{(q_m - q^*)\,C^*}{q^*} \quad (2)$$

where q_m is the immunosorbent's static binding capacity, q^* is the concentration of the immunocomplex formed ([Ab · Ag] in eqn. 1) in equilibrium with C^*, which is the [Ag] remaining in solution. The concentration of functionally effective, unoccupied antibody binding sites is represented by $q_m - q^*$ or [Ab] in eqn. 1.

In theory, for efficient antigen capture, [Ag] should be much greater than K_{de}. The capture effi-

0021-9673/92/$05.00

ciency would be expected to decrease when [Ag] < K_{de}. A typical K_{de} for antigen–antibody interaction in an agarose-based immunosorbent is *ca.* $1.5 \cdot 10^{-8}$ *M* [2].

The kinetic apects of MIC were investigated with the aim of developing efficient systems for recombinant protein purification. In these studies, the effects of mass transfer rate, feed-stream [Ag] and antibody binding-site concentration were determined in relation to the membrane's capture efficiency.

EXPERIMENTAL

Materials

Hollow-fiber membrane modules (hydrazide) were provided by Sepracor (Marlborough, MA, USA). Monoclonal antibodies LI-8, 5B1 and humanized anti-Tac (anti-Tac-H) and recombinant human interferon-α2a (rIFN-α2a) were all prepared in-house. *Escherichia coli* cells expressing recombinant human interleukin-2 (rIL-2) and rIFN-α2a, and CHO-conditioned media containing interleukin-2 receptor (IL-2R), were obtained from the Bioprocess Development Department, Hoffmann-La Roche (Nutley, NJ, USA). NuGel-HZ and Affi-Gel-HZ were purchased from Separation Industries (Metuchen, NJ, USA) and Bio-Rad Labs. (Richmond, CA, USA), respectively. Sodium metaperiodiate and sodium cyanoborohydride were obtained from Sigma (St. Louis, MO, USA) and concentrated phosphate buffered saline (10 × PBS) was purchased from Whittaker Bioproducts (Walkersville, MD, USA). All other chemicals were of analytical-reagent grade.

Model immunoaffinity system

The antigen was recombinant human interferon-α2a (rIFN-α2a). The immunosorbent consisted of a 0.4-ml hydrazide-derivatized hollow-fiber membrane to which 7.02 mg of LI-8 (monoclonal antibody to rIFN-α2a) was immobilized in an oriented fashion, via the sugar moieties in the F_c region of the IgG molecule [3–5]. The coupling reaction scheme is shown in Fig. 1.

Oxidation of antibody was carried out at pH 5.5 in the presence of 0.1 *M* sodium metaperiodate. A desalting step was used to remove unreacted periodate. The oxidized antibody was then allowed to react with the hydrazide membrane and the hydrazone bond thus formed was further stabilized by sodium cyanoborohydride reduction. The static binding capacity of the membrane was experimentally determined to be 0.437 mg of rIFN-α2a.

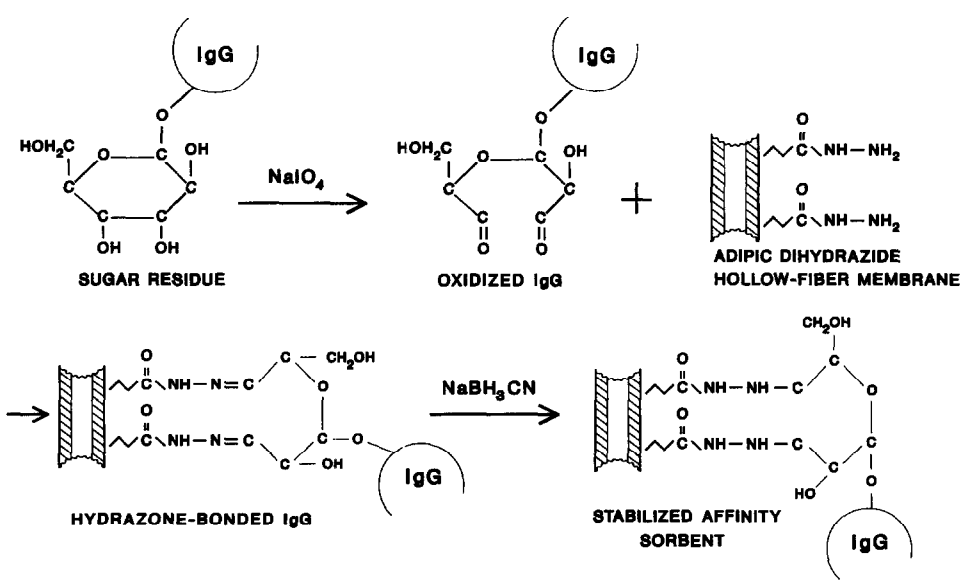

Fig. 1. Reaction scheme for oriented coupling of IgG to hydrazide membrane.

Mass transfer rate: fluid residence time vs. antigen capture

A 25-ml volume of a 22 μg/ml rIFN-α2a solution in PBS was loaded on to the model system at flow-rates of 2.5, 25, 50 and 100 ml/min. Dynamic binding capacities and capture efficiencies were determined. The fluid residence time, t_R, was calculated from the equation

$$t_R = \frac{\text{membrane volume (ml)} \cdot 60}{\text{filtrate flow-rate (ml/min)}}$$

Adsorption kinetics

Antigen concentration, [Ag], vs. capture efficiency. Dynamic binding capacities and capture efficiencies were determined for the model system at feed-stream antigen (rIFN-α2a) concentrations of 0.1, 1, 10 and 100 μg/ml, corresponding to 5.2, 52, 520 and 5200 n*M*, respectively. In each experiment, a total of 0.55 mg of rIFN-α2a was loaded at a fixed flow-rate of 5 ml/min (fluid residence time 4.8 s).

Antibody concentration, [Ab], vs. binding efficiency. Seven immunoaffinity membranes with various LI-8 coupling densities were prepared. The expected binding capacities were calculated taking into account a 2:1 stoichiometry for antigen–antibody binding. Observed (static) binding capacities were determined and expressed as percentages of the expected values (*i.e.*, binding efficiencies).

Antigen breakthrough point. The hollow-fiber membrane-NuGel- and Affi-Gel-based immunosorbents used contained 2.75, 1.68 and 1.67 mg of immobilized LI-8, respectively, and had corresponding static binding capacities of 0.307, 0.179 and 0.241 mg of rIFN-α2a. A 40-ml volume of 25 μg/ml rIFN-α2a solution in PBS was loaded on to each support at a flow-rate of 2 ml/min. One-minute fractions were collected throughout the loading step. The absorbance (A_{280}) of each fraction was determined and expressed as a percentage of the feedstream UV absorbance. These percentages, representing unbound antigen in the breakthrough material, were plotted against the cumulative amount of antigen passed through the immunosorbent up to and including the given fraction. Breakthrough points (%) are given in terms of the immunosorbents' static binding capacities.

Recombinant protein purification

rIFN-α2a. A 50-ml volume of *E. coli* extract (7.7 μg/ml rIFN-α2a) was loaded on to an LI-8 immunoaffinity membrane (0.4 ml) with a static binding capacity of 200 μg of rIFN-α2a. Extraction and purification were carried out as described elsewhere [6].

Interleukin-2 (rIL-2). A hollow-fiber membrane to which 5B1 (monoclonal antibody to rIL-2) was immobilized was used to purify rIL-2 from 100 ml of crude *E. coli* extract (*ca.* 10 μg/ml rIL-2). The static binding capacity of the membrane for rIL-2 was 357 μg. See ref. 7 for experimental details.

Interleukin-2 receptor (IL-2R). A 500-ml volume of crude cell culture media (*ca.* 2 μg/ml IL-2R) was applied to a 0.4-ml membrane immunosorbent containing anti-Tac-H (humanized monoclonal antibody to IL-2R). The static binding capacity of the immunosorbent was 201 μg of IL-2R. The washing and elution procedures were the same as in rIL-2 purification.

All three purified proteins were analysed by sodium dodecyl sulfate–polyacrylamide gel electrophoresis (SDS-PAGE) under reducing conditions according to Laemmli's method [8], and were subjected to bioassays.

Large scale rIL-2 purification. A 9.7 ml hollow-fiber membrane to which 29 mg 5B1 was immobilized, was used to process 500 ml *E. coli* extract (*ca.* 10 μg/ml rIL-2) at a filtrate flow-rate of 140 ml/min during loading. Subsequent steps were carried out at 200 ml/min. The membrane's static binding capacity was 5 mg rIL-2. Purified material was subjected to SDS-PAGE analysis and bioassay.

RESULTS AND DISCUSSION

As illustrated in Fig. 2, the antigen capture efficiencies of the model immunoaffinity membrane gradually decrease from 64 to 40% as the fluid residence times, t_R, are reduced from 9.6 to 0.24 s. Despite the 40-fold reduction in t_R, the observed decrease in membrane capture efficiency is relatively small. Even at an adsorption flow-rate of 100 ml/min, corresponding to a residence time of only 0.24 s, an effective capture efficiency (40%) is still maintained. Further, the fact that such high flow-rates could be achieved with such a small membrane (0.4-ml volume) clearly demonstrates its excellent mass transfer capabilities. In an efficient affinity purification system, the diffusion time $t_D \ll t_R$. In the hol-

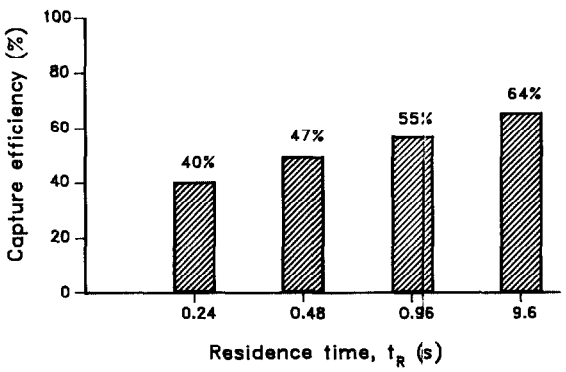

Fig. 2. Effect of fluid residence time on antigen capture efficiency. Residence times were calculated as described under Experimental. Capture efficiency is the dynamic binding capacity expressed as a percentage of static binding capacity.

low-fiber membrane used in this study, with a diffusional distance of *ca.* 0.4 μm, t_D is *ca.* 16 ms, which is far below even the shortest fluid residence time investigated. Therefore, negligible mass transfer limitations were exhibited by the membrane. However, the observed decrease in antigen capture implies some potential kinetic limitations in membrane-based affinity systems, which may become more apparent as t_R approaches the association time of the proteins involved.

The results in Table I show that a three orders of magnitude change in feed-stream antigen concentration (from 0.1 to 100 μg/ml) produces comparatively little change in antigen capture efficiencies (range 46–61%). As expected, when [Ag] is much greater than the effective dissociation constant (K_{de} for typical Ag–Ab interaction $\approx 15 \cdot 10^{-9}$ *M*), the efficiencies are significantly higher than when [Ag] is below K_{de}. For example, efficiencies of 56–61% were observed for [Ag] = 52–5200 n*M*, compared with only 46% when [Ag] = 5.2 n*M*. However, even at [Ag] < K_{de}, an effective capture efficiency of 46% is still maintained. It should be pointed out that the feed-stream [Ag] of crude recombinant proteins is generally in the range 1–10 μg/ml, which corresponds to concentrations considerably higher than the K_{de} value for these protein interactions.

Although eqn. 1 predicts that binding capacities should increase proportionately to [Ab], the results shown in Table II indicate otherwise. At high concentrations of immobilized antibody (83–110 nmol/ml), reduced binding efficiencies (26–33%) can be attributed to an increase in steric hindrance due to antibody crowding. This is further illustrated by the near-theoretical binding efficiencies (up to 90%) achieved with low antibody coupling densities (2–5 nmol/ml), in which crowding is minimized.

As demonstrated in Fig. 3, antigen breakthrough in the membrane occurred at 80% of its static binding capacity, compared with 67% and 39% for Nu-Gel and Affi-Gel, respectively. The high capture efficiency of the membrane is primarily attributed to its short diffusional distance and lack of diffusional limitations, which facilitate antibody accessibility. Thus, antigen breakthrough in the membrane is

TABLE I

EFFECT OF FEED-STREAM [Ag] ON CAPTURE EFFICIENCY

Capture efficiencies of an immunoaffinity membrane (static binding capacity, 0.437 mg of rIFN-α2a) were determined for various feed-stream antigen (rIFN-α2a) concentrations. $K_{de} \approx 1.5 \cdot 10^{-8}$ *M* for typical Ag–Ab interaction.

Feedstream [Ag]		Capture efficiency (%)
μg/ml	n*M*	
0.1	5.2	46
1	52	61
10	520	57
100	5200	56

TABLE II

EFFECT OF ANTIBODY CONCENTRATION, [Ab], ON BINDING EFFICIENCY

Antigen (rIFN-α2a) binding capacities and efficiencies of seven immunoaffinity membranes with increasing LI-8 coupling densities were determined. Binding efficiency is the observed binding capacity expressed as a percentage of the expected value, which was calculated assuming a 1:2 antibody–antigen binding stoichiometry.

[Ab] (nmol/ml)	Binding capacity (nmol/ml)		Binding efficiency (%)
	Expected	Observed	
2.4	4.8	4.3	90
4.7	9.4	7.6	81
8.9	17.8	8.2	46
15.8	31.6	15.2	48
31.0	62.0	26.0	42
83.4	166.8	54.7	33
110.1	220.2	56.9	26

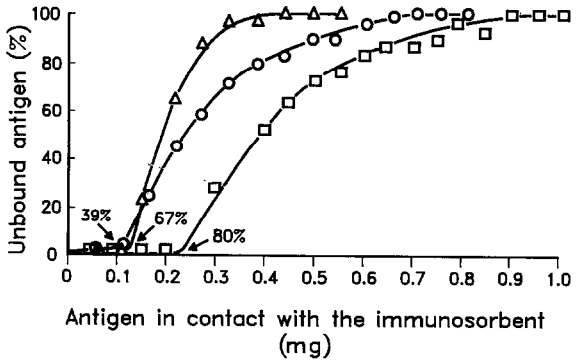

Fig. 3. Antigen (rIFN-α2a) breakthrough curves for (□) hollow-fiber membrane-, (△) NuGel- and (○) Affi-Gel-based LI-8 immunosorbents. Percentage of unbound antigen in the breakthrough material is plotted against the corresponding amount of antigen in contact with the immunosorbent up to that point. Antigen breakthrough points of the various immunosorbents occurred at (○) 39%, (△) 67% and (□) 80% of their respective static binding capacities.

mainly a result of diminished binding site availability with continued immunocomplex formation. The steric hindrance caused by the increased relative molecular mass of the immunocomplex formed also contributes to the continually decreasing adsorption rate observed after the breakthrough point. In contrast, the stretched S-shape of the breakthrough curves for gels reflects mass transfer limitations in addition to depletion of available antibody sites. The overall decrease in antigen capture rate illustrated by these curves as the concentration of antibody sites, [Ab], is progressively reduced was predicted by eqn. 1.

After studying the kinetic aspects of membrane-based immunoaffinity chromatography and determining its capabilities and limitations using the model LI-8–rIFN-α2a system, it was necessary to demonstrate the utility of MIC in recombinant protein purification on both small and large scales. The three proteins chosen for small-scale purification (0.4-ml membrane volume) were rIFN-α2a, rIL-2 and IL-2R, which differ in origin and physical, biochemical and biological characteristics (Table III).

The protein recoveries were nearly equivalent to the static binding capacities of the respective immunosorbents. All three proteins were recovered with >95% purity as indicated by SDS-PAGE (Fig. 4). The purified materials were biologically active according to the results of specific bioassays (data not

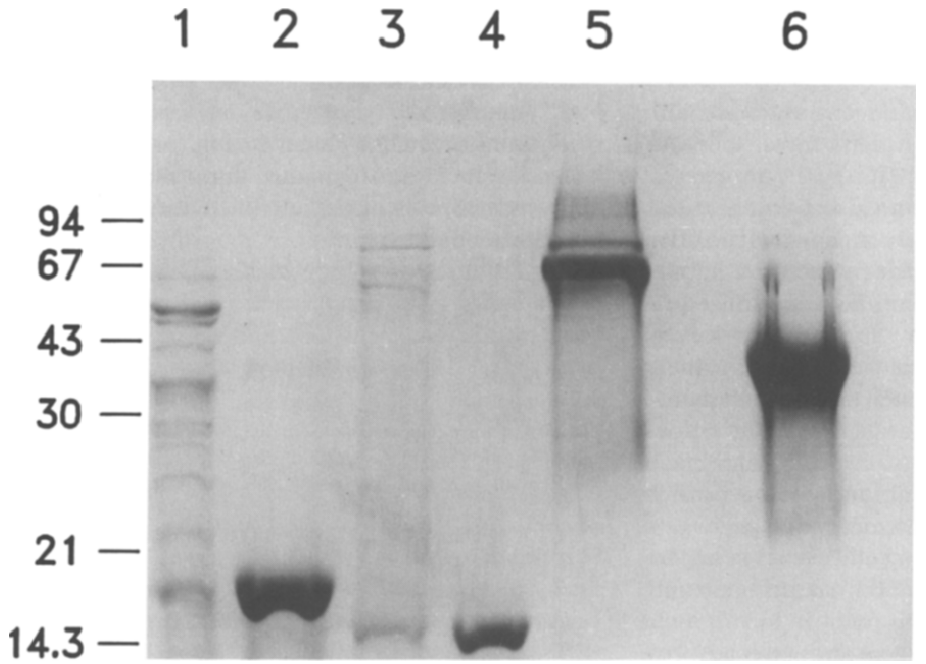

Fig. 4. SDS-PAGE of MIC-purified proteins. Standard molecular mass markers are shown on the left ($M_r \cdot 10^{-3}$). Lanes: 1 and 2 = crude and purified rIFN-α2a; 3 and 4 = crude and purified rIL-2; 5 and 6 = crude and purified IL-2R.

TABLE III

MIC-PURIFIED RECOMBINANT PROTEINS

Physical, biochemical and biological properties of interferon, interleukin-2 and interleukin-2 receptor.

Protein	M_r	Characterization	Immunosorbent	Starting material
rIFN-α2a	$19.2 \cdot 10^3$	Polypeptide, anti-viral protein	LI-8 monoclonal antibody	*E. coli* extract
rIL-2	$15.5 \cdot 10^3$	Lymphokine, immunomodulator	5B1 monoclonal antibody	*E. coli* extract
IL-2R	$43.0 \cdot 10^3$	Glycoprotein, *ca.* 50% sugar	Humanized anti-Tac	CHO-conditioned cell culture media

shown). The diversity of the three proteins may imply a universal applicability of MIC.

The large-scale rIL-2 purification (9.7-ml membrane volume) yielded 4.63 mg of rIL-2, corresponding to a capture efficiency of 93%. These results emphasize the virtual lack of diffusional limitations in the hollow-fiber membrane. Despite the short fluid residence time (4 s) and low feed-stream antigen concentration (*ca.* 10 μg/ml), high rIL-2 recovery and purity were achieved. Hence, the mass transfer advantages afforded by the membrane and the fast antigen–antibody adsorption kinetics could be taken advantage of to the fullest extent.

CONCLUSIONS

It has been shown that antigen–antibody adsorption kinetics, rather than mass transfer, is the initial rate-limiting factor in MIC. In the absence of diffusional limitations, immunoadsorption is at the limits of the antigen–antibody kinetics. Hence the high-affinity interactions which characterize immunoaffinity chromatography can be fully utilized in membranes. Antigen capture remains effective even at extremely short fluid residence times. Further, binding is not kinetically limited at feed-stream antigen concentrations less than K_{de} and far below those usually associated with crude recombinant proteins. Therefore, the membrane's mass transfer advantages are effectively utilized.

The near-theoretical binding efficiencies achieved at low concentrations of immobilized antibody and the late antigen breakthrough point in membranes both demonstrate that antigen–antibody adsorption kinetics are not mass transfer limited in the membrane system. However, the fact that antigen binding becomes less effective with increased antibody densities, together with the S-shaped character of the breakthrough curve (assuming uniform fluid flow), together point to the role of steric hindrance in reducing the absolute amount and overall rate of antigen capture. Steric hindrance, which can be expected in any immobilized system, is perhaps the main factor which separates a membrane-based system from free-solution conditions.

Overall, the kinetic aspects of membrane-based immunoaffinity chromatography render it a highly efficient system, well suited for the industrial-scale production of recombinantly produced biotherapeutics.

ACKNOWLEDGEMENTS

The author thanks Pascal Bailon for his support, encouragement and guidance during the course of this study. She is also grateful to Lisa Nieves for typing the manuscript.

REFERENCES

1 S. Brandt, R. A. Goffe, S. B. Kessler, J. L. O'Connor and S. E. Zale, *Bio/Technol.*, 6 (1988) 779.
2 H. A. Chase, *Chem. Eng. Sci.*, 39 (1984) 1099.
3 A. Rothfus and E. L. Smith, *J. Biol. Chem.*, 238 (1963) 1402.
4 R. Jost, T. Miron and M. Wilchek, *Biochim. Biophys. Acta*, 362 (1974) 75.
5 D. J. O'Shannessy and M. Wilchek, *Anal. Biochem.*, 191 (1990) 1.
6 S. J. Tarnowski, S. K. Roy, R. A. Liptak, D. K. Lee and R. Y. Ning, *Methods Enzymol.*, 119 (1986) 153.
7 P. Bailon, D. V. Weber, R. F. Keeney, J. E. Fredericks, C. Smith, P. C. Familletti and J. E. Smart, *Bio/Technol.*, 5 (1987) 1195.
8 U. K. Laemmli, *Nature (London)*, 227 (1970) 680.